



Hepatoprotective Efficacy and Interventional Mechanism of Qijia Rougan Decoction in Liver Fibrosis

Xiao-Feng Chen[†], Yumei Wang[†], Shaoxiu Ji[†], Xin Sun, Quansheng Feng, Han Yu* and Chao Liu*

School of Basic Medical Sciences, Chengdu University of Traditional Chinese Medicine, Chengdu, China

OPEN ACCESS

Edited by:

Rolf Teschke,
Hospital Hanau, Germany

Reviewed by:

Mamdouh M. El-Shishtawy,
Mansoura University, Egypt
Mingyu Sun,
Shanghai University of Traditional
Chinese Medicine, China
Xue Xiaoyong,
Beijing University of Chinese Medicine,
China

*Correspondence:

Han Yu
yuhan@cduetcm.edu.cn
Chao Liu
liuchao@cduetcm.edu.cn

[†]These authors have contributed
equally to this work

Specialty section:

This article was submitted to
Gastrointestinal and Hepatic
Pharmacology,
a section of the journal
Frontiers in Pharmacology

Received: 02 April 2022

Accepted: 24 May 2022

Published: 01 July 2022

Citation:

Chen X-F, Wang Y, Ji S, Sun X, Feng
Q, Yu H and Liu C (2022)
Hepatoprotective Efficacy and
Interventional Mechanism of Qijia
Rougan Decoction in Liver Fibrosis.
Front. Pharmacol. 13:911250.
doi: 10.3389/fphar.2022.911250

Liver fibrosis is a leading contributor to chronic liver diseases such as cirrhosis and liver cancer, which pose a serious health threat worldwide, and there are no effective drugs to treat it. Qijia Rougan decoction was modified from *Sanjiasan*, a traditional Chinese medicine (TCM) described in the “Wenyilun” manuscript. Qijia Rougan decoction possesses hepatoprotective and antifibrotic effects for clinical applications. However, its underlying mechanisms remain largely unknown. In this study, fibrotic rats induced by carbon tetrachloride (CCl₄) were treated with two doses of Qijia Rougan decoction. Histopathological and serum biochemical analyses were carried out to assess liver structure and function, respectively. High-performance liquid chromatography (HPLC) coupled with mass spectrometry (MS) was performed to identify bioactive compositions in Qijia Rougan decoction. Transcriptome analysis using mRNA-sequencing (mRNA-Seq) was used to explore the underlying mechanisms and verified by quantitative real-time polymerase chain reaction (qRT-PCR) and Western blotting. Qijia Rougan decoction significantly attenuated CCl₄-induced hepatic fibrotic injury, supported by promoted liver function and improved liver fibrosis. Eight main representative components originating from raw materials in the Qijia Rougan decoction were found to possess an antifibrotic role. Mechanistically, Qijia Rougan decoction regulated biological processes such as oxidation–reduction, fatty acid metabolism, cell adhesion, and transforming growth factor beta (TGFβ) signaling. We determined that Qijia Rougan decoction reversed the expression of inflammatory cytokines and inhibited the activation of fibrosis-related TGFβ signaling. It also reversed the deterioration of liver structure and function in rats induced by CCl₄. Overall, Qijia Rougan decoction significantly mediated metabolism-associated processes, inhibited inflammatory reactions, and repressed fibrosis-related TGFβ signaling, which prevented liver fibrosis deterioration. Our study deepens our understanding of TCM in the diagnosis and treatment of liver fibrosis.

Keywords: qijia rougan decoction, liver fibrosis, transcriptomics, transforming growth factor beta, inflammation

INTRODUCTION

Liver fibrosis is a collective pathological process present in most chronic liver diseases, including viral hepatitis, alcoholic liver disease (ALD), and non-alcoholic fatty liver disease (NAFLD) (Pellicoro et al., 2014; Schwabe et al., 2020; Friedman and Pinzani, 2022), and is a global health burden causing high morbidity and mortality. Short-term liver fibrosis is considered a reversible and protective reaction to hepatic damage (Kisseleva and Brenner, 2021). Long-term liver fibrosis can lead to cirrhosis and even liver cancer. Liver fibrosis is characterized by excessive deposition of extracellular matrix (ECM) in the liver (Schuppan et al., 2018; Parola and Pinzani, 2019; Xu et al., 2019). The activated hepatic stellate cells (HSCs) primarily account for producing the ECM (Mu et al., 2018). Various injurious stimuli lead to activation of quiescent hepatic stellate cells (HSCs) to yield excessive ECM, which damages the structure and function of the liver (Gao et al., 2020; Chen et al., 2021). Active and effective interventions are expected to delay or prevent the progression of liver fibrosis, prolong patient survival, improve the quality of life, and prevent the deterioration of chronic liver diseases. Thus, reversal or inhibition of liver fibrosis has become a key target in the treatment of liver diseases.

Although there is currently no effective Western medicine for treating liver fibrosis, traditional Chinese medicine (TCM) shows efficient advantages in treating liver fibrosis (Feng et al., 2009; Li, 2020). For example, Xiaoyaosan decoction, containing eight Chinese herbs, was reported to prevent the progression of liver fibrosis induced by CCl₄ in rats, which was mediated through transforming growth factor beta1 (TGFβ1)/Smad signaling cascades (Zhou et al., 2021). Ganshuang granules, a prepared TCM decoction, can regulate gut microbiota composition and diversity to maintain intestinal integrity and exert antioxidant and anti-inflammatory effects, therefore repressing liver fibrosis (Zhao et al., 2021). Yiguanjian decoction, a representative TCM comprising six medicinal herbs, inhibits liver fibrosis by maintaining the resting state of hepatic stellate cells and hepatocyte viability (Li et al., 2019), repressing liver angiogenesis (Zhou et al., 2015), and modulating inflammatory cytokine release from macrophages (Xu et al., 2021). Due to the multicomponent, multitarget, and multifunction nature of TCM, along with its infrequency of side-effects and drug-resistance induction, the prospect of using TCM to treat liver fibrosis is promising.

Qijia Rougan decoction (QJ) was modified from *Sanjiasan*, found in the “Wenyilun” manuscript and documented to treat lumps in the body during the Ming dynasty. Our previous study demonstrated that another formula, called Fuzheng Xiaozheng prescription (FZXZP), derived from *Sanjiasan*, efficiently inhibited hepatocellular carcinoma (Li X. et al., 2022). Based on the abovementioned research, Qijia Rougan decoction was developed, containing 10 herbs, namely, *Astragalus mongholicus* Bunge, *Angelica sinensis* (Oliv.) Diels, *Trionyx sinensis* Wiegmann, *Eupolyphaga seu Steleophaga*, *Salvia miltiorrhiza* Bunge, *Carthamus tinctorius* L., *Prunus persica* (L.) Batsch, *Sparganium stolonierum*, Buch., *Curcuma phaeocaulis* Valetton, and *Glycyrrhiza uralensis* Fisch. Among these, *Astragalus*

mongholicus Bunge was the sovereign drug to enhance qi and has been demonstrated to exert an antifibrotic role (Yang et al., 2008); *Carapax Trionycis*, *Eupolyphaga seu Steleophaga*, *Salvia miltiorrhiza* Bunge, *Carthamus tinctorius* L., and *Prunus persica* (L.) Batsch were ministerial drugs to invigorate blood and nourish Yin and could retard liver fibrosis (Tan et al., 2006; Hu et al., 2017; Li X. et al., 2022); and *Angelica sinensis* (Oliv.) Diels, *Sparganium stolonierum*, Buch., and *Curcuma phaeocaulis* Valetton were adjuvant medicines to expel blood stasis and possessed a hepatoprotective role (Ali et al., 2018). *Glycyrrhiza uralensis* Fisch. was a conductant drug to regulate medicinal nature. Together, the mixture of Qijia Rougan decoction could reinforce qi, activate blood circulation, remove blood stasis, and dredge collaterals, which together were effective for treating liver fibrosis. Moreover, modern pharmacological studies have shown that almost all the aforementioned traditional Chinese medicines show antifibrotic effects by modulating inflammation and immune responses, inhibiting the activation of hepatic stellate cells (HSCs), and repressing pro-fibrotic signaling pathways (Hu et al., 2017; Ali et al., 2018; Liu and Lv, 2020). However, the role of Qijia Rougan decoction on liver fibrosis and its underlying mechanisms remain to be explored.

In the present study, the rat liver fibrosis model was established by CCl₄ injection and validated by serum biochemical analyses, liver histopathologic changes, liver collagen, and fibrosis-associated gene expression. We found that Qijia Rougan decoction significantly inhibited CCl₄-induced liver fibrosis and maintained the integrity of the liver by regulating the expression of inflammation-related genes and modulating transforming growth factor beta (TGFβ) signaling. Collectively, these findings indicate that Qijia Rougan decoction is a promising therapeutic option for treating fibrosis-related liver damage.

MATERIALS AND METHODS

Animals

We purchased 56 healthy male Sprague–Dawley (SD) rats weighing 160–200 g from Chengdu Dossy Experimental Animals Co., Ltd. (Chengdu, China; certification no. SCXK-CHUAN, 2020-030). The rats were kept in a standard 12 h light–dark cycle and allowed free access to water and food. All animal protocols were approved by Ethics Committee of Chengdu University of Traditional Chinese Medicine, and the rat experiments were consistent with the guidelines of the National Institutes of Health (United States).

Qijia Rougan Decoction Preparation

All herbs were obtained from Hospital of Chengdu University of Traditional Chinese Medicine. Qijia Rougan decoction (QJ) consisted of 10 herbal medicines, including eight herbs and two animal drugs. Information on the herbs is presented in **Table 1**. We prepared the 10 herbal medicines following the National Pharmacopeia standards. All eight herbs were soaked in purified water for 30 min. The two animal drugs were soaked in

TABLE 1 | The composition of Qijia Rougan decoction.

Chinese name	English name	Botanical name ^a	Family	Weight (g)	Part used	Herbal-producing region
Huang Qi	Astragalus	<i>Astragalus mongholicus</i> Bunge	Leguminosae	30	Root	Gansu
Dang Gui	Chiretta	<i>Angelica sinensis</i> (Oliv.) Diels	Apiaceae	9	Root	Gansu
Bie Jia	Carapax trionycis	<i>Trionyx sinensis</i> Wiegmann	Trionychidae	15	Carapace	Hubei
Tu Bie Chong	Ground beetle	<i>Eupolyphaga seu</i> Steleophaga	Polyphagidae	12	Insect body	Anhui
Dan Shen	Salvia miltiorrhiza	<i>Salvia miltiorrhiza</i> Bunge	Lamiaceae	18	Root	Shandong
Hong Hua	Safflower	<i>Carthamus tinctorius</i> L.	Compositae	18	Flower	Xinjiang
Tao Ren	Semen persicae	<i>Prunus persica</i> (L.) Batsch	Rosaceae	18	Seed	Gansu
San Leng	Rhizoma sparganii	<i>Sparganium stolonierum</i> , Buch.	Typhaceae	15	Tuber	Anhui
E Zhu	Acrogenous turmeric rhizome	<i>Curcuma phaeoacaulis</i> Valetton	Zingiberaceae	15	Rhizome	Sichuan
Gan Cao	liquorice	<i>Glycyrrhiza uralensis</i> Fisch.	Leguminosae	6	Root and rhizome	Xinjiang

^aThe plant name has been checked with <http://www.theplantlist.org>.

TABLE 2 | mRNA primer sequences.

Gene names	Forward primer (5'-3')	Reverse primer (5'-3')
<i>Cxcl12</i>	TGTTGACCCCGGACACCTAA	TGGCGCCCAAGGGAAT
<i>Cxcl1</i>	CAGACAGTGGCAGGGATTCA	CCTGGCGGCATCACCTT
<i>Tgfb1</i>	GAAACGGGAAGCGCATCGA	CTGGCAGCCTTAGTTTGGGA
<i>Tgfb2</i>	TCATCCCAATAAGAGCCAAGAG	TGGAGGTGCCATCGATACCT
<i>Tgfb3</i>	GCGCCCOCTCTACATTGAC	GGTTCGTGGACCCATTTC
<i>Tgfb11</i>	CGCTTCTCCCCACGATGT	AAGCGCGTGACATTTTATGTC
<i>Col1a1</i>	GTACATCAGCCCAAAACCCCA	CAGGATCGGAACCTTCGCTT
<i>Timp1</i>	GACACGCTAGAGCAGATACCA	CCAGGTCCGAGTTGCAGAAA
<i>Gapdh</i>	GTGATGGGTGTGAACCCAGAG	GTCCATGAGCCCTCCACGATG

purified water for 50 min, and then about 1.5 L of purified water was added and the animal drugs were boiled for 30 min. Then, the eight remaining herbs were added and were allowed to boil for 30 min. The drug solution was filtered, and the abovementioned process was repeated. Finally, the filtered drug solution was concentrated and stored for subsequent use.

Animal Experiments

The rats were randomized to four groups: control group (Control); CCl₄ group (Model), receiving CCl₄ from week 0–15; QJ low-dose group (QJ-L), receiving oral QJ (7.0 g/kg) from weeks 9–15 and CCl₄ from week 0–15; and QJ high-dose group (QJ-H), receiving oral QJ (28.0 g/kg) from weeks 9–15 and CCl₄ from week 0–15. The rats received CCl₄ *via* subcutaneous injection of 50% CCl₄ olive oil twice a week. Then, beginning at week 9, 400 μl QJ was orally administered daily to the QJ-L and QJ-H groups. Finally, the rats were anesthetized, and their serum was obtained through abdominal aortic blood collection. The rats were then euthanized, and their livers were immediately collected for dissection and subsequent analysis.

Quantitative Real-Time Polymerase Chain Reaction

Total RNA in the rat liver was extracted using TRIzol (Invitrogen). Then, a First-Strand cDNA Synthesis kit (New England Biolabs, #M0277) was used to synthesize the first-strand cDNA. qRT-PCR was carried out with a SYBR Green

Master Mix (TaKaRa, #R820A) to detect the relative mRNA levels of the indicated genes. The expressions of *Cxcl12*, *Cxcl1*, *Tgfb1*, *Tgfb2*, *Tgfb3*, *Tgfb11*, *Col1a1*, and *Timp1* were detected. *Gapdh* was applied as an internal control. Sequences of qRT-PCR primers are shown in **Table 2**. Gene expression was calculated by the $2^{-\Delta\Delta CT}$ method.

Histological Staining

Fresh rat livers were fixed in 4% paraformaldehyde. Fixed livers were embedded in paraffin and then cut into 5-μm sections. Liver sections were stained with hematoxylin–eosin (H&E) or Masson's staining to identify liver structure and the state of collagen accumulation, respectively. A quantitative digital image analysis system (Image-Pro Plus 6.0) was used to analyze the histological staining images.

Immunohistochemical Staining

For immunohistochemical (IHC) staining, paraffin-embedded liver sections were deparaffinized with xylene and rehydrated with a gradient of ethanol. Endogenous peroxidases were quenched by 3% hydrogen peroxide (H₂O₂) for half an hour. EDTA-Tris (pH 8.0) was used to boil the sections for 3 min for antigen retrieval. The sections were blocked with goat serum to block nonspecific staining of the liver and incubated with individual primary antibodies α-SMA (Servicebio, GB111364) and collagen I (Servicebio, GB11022) overnight at 4°C. Finally, diaminobenzidine (DAB) staining was performed and counterstained with hematoxylin.

Western Blotting

The protein was isolated with RIPA lysis buffer (Beyotime, #P0013B) containing a protease inhibitor cocktail and phosphatase inhibitor as previously described (Tang et al., 2017). The liver homogenate was sonicated and centrifuged at 4°C for 15 min to collect the supernatant for Western blotting. Then, the concentration of every supernatant protein was evaluated by the BCA Protein Assay Reagent (Thermo, #23227). Eventually, the supernatant protein was mixed with SDS-PAGE Sample Loading Buffer (Beyotime Biotechnology, #P0015) and boiled in water to denature the protein. 20 µg of protein was subjected to SDS-PAGE and transferred to a PVDF membrane. Five percent non-fat milk was used to block the PVDF membrane. Then, the membrane was incubated with individual primary antibodies overnight at 4°C. Subsequently, the membrane was incubated with a horseradish peroxidase-conjugated secondary antibody (ZSGB-BIO; #ZB2301, #ZB2305), and protein expression was detected by Pierce ECL Western Blotting Substrate (Thermo, #32106). Antibodies to p-SMAD3 (CST, 9520), SMAD3 (Proteintech, 66516-1-Ig), p-SMAD2 (CST, 3108), SMAD2 (CST, 5339), TGF-βR1 (Servicebio, GB11271), TGF-βR2 (Servicebio, GB112244), TGF-β (bioworlde, BS1361), and GAPDH (abcam, ab8245) were used in this study.

HPLC-MS/MS Analysis

High-performance liquid chromatography (HPLC) tandem mass spectrometry (MS) was performed for quality control. Briefly, the Qijia Rougan decoction was mixed with 1 ml of methanol: water (4:1, v/v), vortexed for 10 min, and centrifuged for 10 min at 4°C and 20,000 g. The supernatant was filtered through a 0.22-µm filter membrane for subsequent HPLC analysis (UltiMate 3000 RS; Thermo Scientific). The analytical column was AQ-C18 with a dimension of 150 mm × 2.1 mm and 1.8 µm particle size (Welch). The mobile phase contained the aqueous phases of 0.1% formic acid and an organic phase of methanol. The chromatography gradients are shown below: 2% methanol at 1 min, 20% methanol at 5 min, 50% methanol at 10 min, 80% methanol at 15 min, 95% methanol at 20 min, 95% methanol at 25 min, 2% methanol at 26 min, and 2% methanol at 30 min. The column was maintained at 35°C. The injection volume was 5 µl, and the flow rate was 0.30 ml/min. MS analysis was carried out on a Q Exactive high-resolution mass spectrometer (Thermo Fisher) with an ESI Source. The MS conditions were spray voltage: 3.8 kV (positive); capillary temperature: 300°C; aux gas heater temperature: 350°C; scanning mode: positive and negative ion switching scanning; scan range: 150.0–2000.0 m/z; resolution: 70,000 full mass, 17,500 dd-MS2; detection mode: full mass/dd-MS2.

Serum Biochemistry Analysis

The concentrations of serum alanine aminotransferase (ALT), aspartate aminotransferase (AST), and total bilirubin (TBIL) were detected with a fully automated biochemical analyzer (Chemray 800, Rayto) according to the manufacturer's instructions in Servicebio. Alanine aminotransferase (ALT, cat. no. GM1102), aspartate aminotransferase (AST, cat. no.

GM1103), and total bilirubin (TBIL, cat. no. GM1105) were purchased from Servicebio. Enzyme-linked immunosorbent assay (ELISA) was used to detect the content of hyaluronic acid (HA), laminin (LN), and type III procollagen (PC-III) in the blood, according to the manufacturer's instructions.

mRNA Sequencing

Total RNA was extracted from liver tissues using TRIzol reagent, as previously described (Tang et al., 2017). A Bioanalyzer 2,100 system (Agilent Technologies, CA, United States) was used to assess RNA integrity. Novogene performed mRNA sequencing. Total RNAs were used as the input material for the RNA sample preparations to prepare the transcriptome sequencing libraries. The clustering of the index-coded samples was performed on a cBot Cluster Generation System, using a TruSeq PE Cluster Kit v3-cBot-HS (Illumina), according to the manufacturer's instructions. After cluster generation, the library preparations were sequenced on an Illumina NovaSeq platform, and 150-bp paired-end reads were generated. Raw data (raw reads) in a fastq format were first processed through in-house Perl scripts. In this step, clean data (clean reads) were obtained by removing reads containing adapters, reads containing ploy-N, and low-quality reads from the raw data. In addition, Q20, Q30, and GC contents were calculated. All downstream analyses were based on clean high-quality data. A corrected *p*-value <0.05 and an absolute fold change ≥1.5 were set as the thresholds for detecting significantly different expression levels. Raw sequence data in this study can be found on the National Center for Biotechnology Information (NCBI) database (<https://www.ncbi.nlm.nih.gov/>) and are available through accession number (PRJNA826993).

Statistical Analysis

All data were presented as mean ± SEM. One-way analysis of variance (ANOVA) was performed to analyze significant differences between the control, model, QJ-L, and QJ-H. *p* values less than 0.05 were considered statistically significant. All statistical analyses were carried out using GraphPad Prism 8.0 or SPSS Version 21 software.

RESULTS

Chemical Components of Qijia Rougan Decoction

In order to preliminarily identify the constituents of Qijia Rougan decoction and explore its antifibrotic role, HPLC-MS/MS analysis was implemented to identify the bioactive components of Qijia Rougan decoction in this study. The total ion current chromatograms (TICCs) of the negative and positive ionization modes of Qijia Rougan decoction are shown in **Figures 1A,B**, respectively. Overall, we identified 1028 components, with 425 components with a >60 mzCloud best-match score in the mzCloud database. We focused on the eight main compounds originating from raw materials in Qijia Rougan decoction with high mzCloud best-match scores >95, namely, ursolic acid, tanshinone IIA, isoliquiritigenin, formononetin, 18-β-glycyrrhetic acid, cryptotanshinone, daidzein, and nicotinic

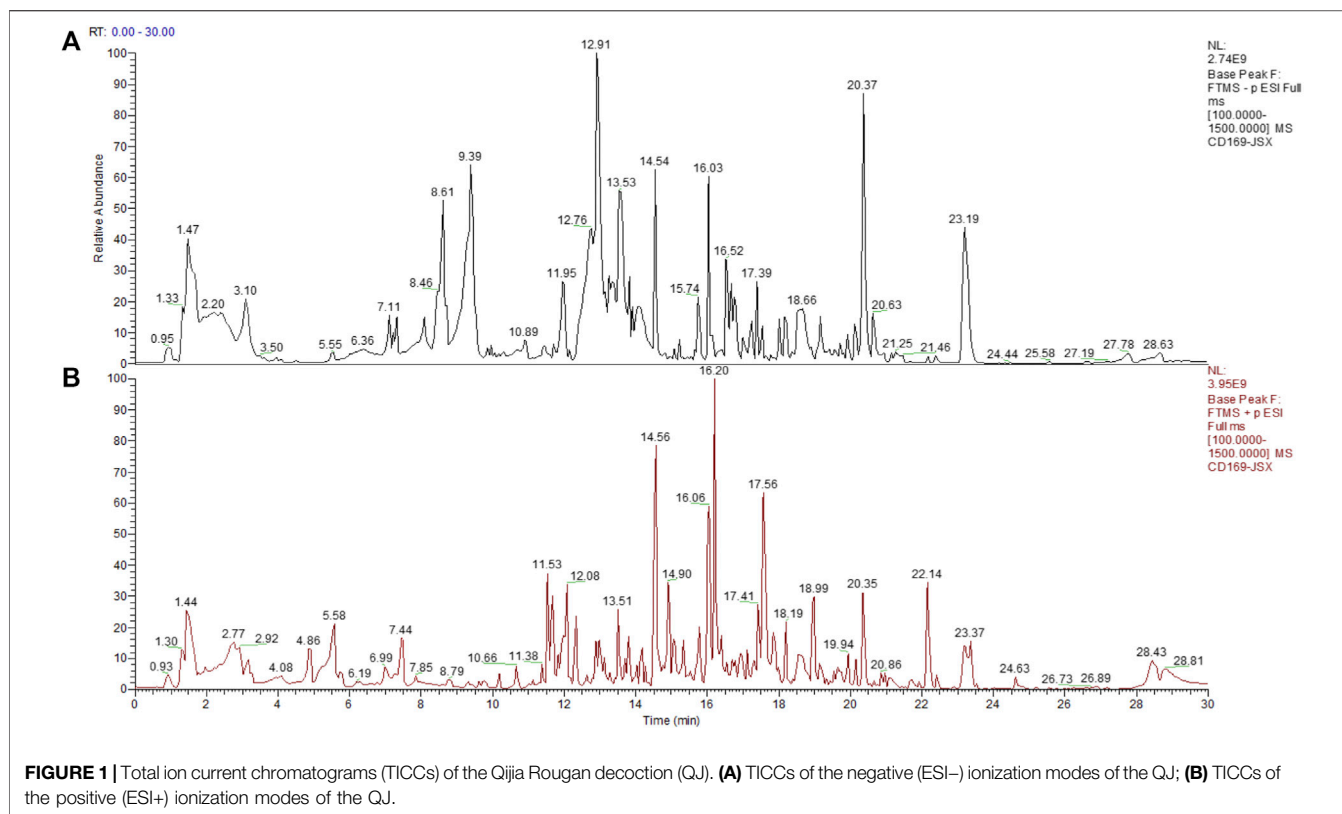


FIGURE 1 | Total ion current chromatograms (TICCs) of the Qijia Rougan decoction (QJ). **(A)** TICCs of the negative (ESI⁻) ionization modes of the QJ; **(B)** TICCs of the positive (ESI⁺) ionization modes of the QJ.

TABLE 3 | Main compounds in Qijia Rougan decoction.

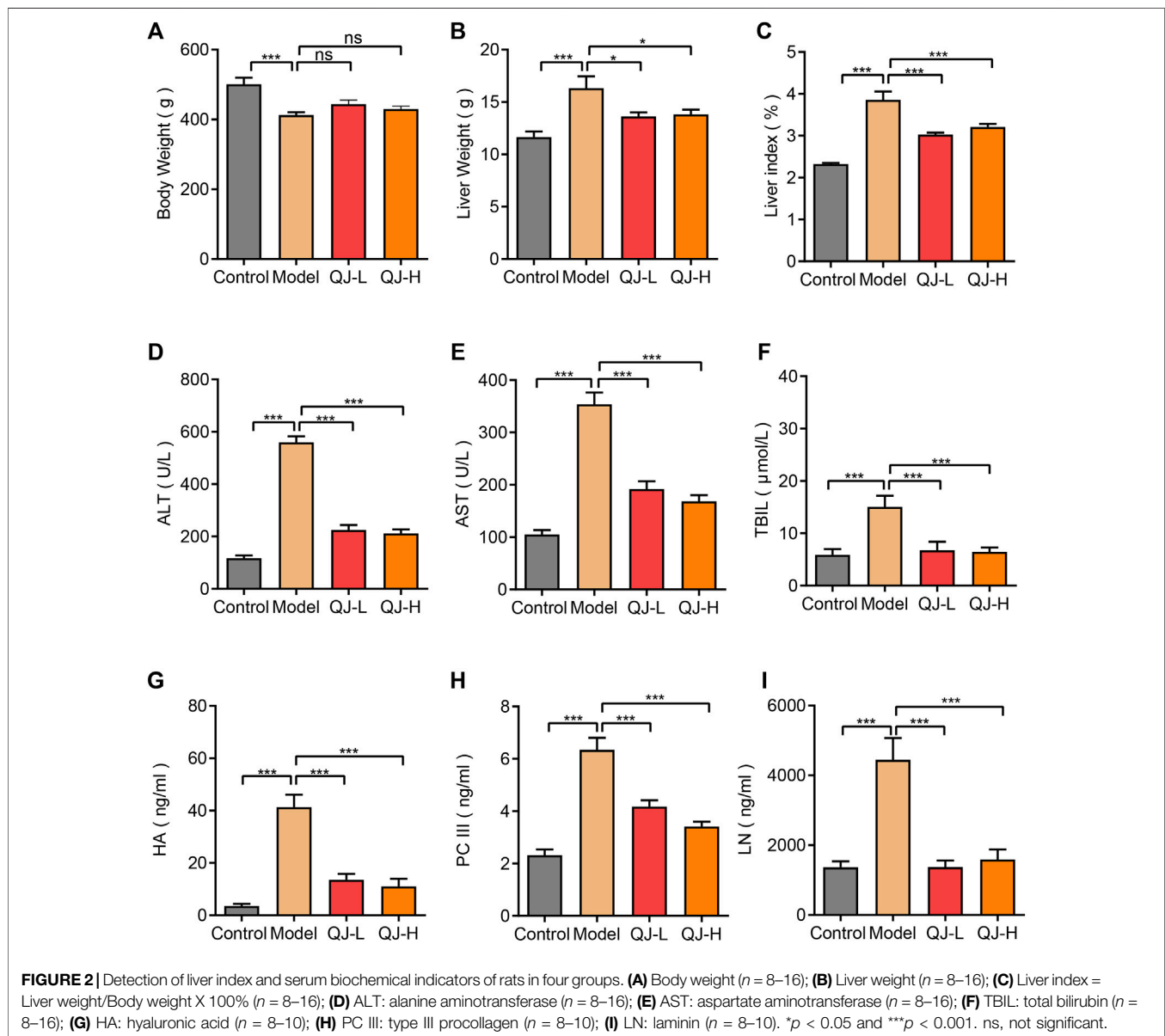
Name	mzCloud best match	Formula	Molecular weight	RT [min]	Area (max.)	Classification
Ursolic acid	97.6	C ₃₀ H ₄₈ O ₃	456.36035	22.161	2876158.66968326	Pentacyclic triterpenoid
Tanshinone IIA	97.5	C ₁₉ H ₁₈ O ₃	294.12493	19.92	67272425.0540303	Diterpenoid naphthoquinone
Isoliquiritigenin	97.4	C ₁₅ H ₁₂ O ₄	256.07273	11.975	112889882.437397	Flavonoid
Formononetin	97.2	C ₁₆ H ₁₂ O ₄	268.07302	16.041	269361987.926751	Isoflavone
18-β-Glycyrrhetic acid	96.9	C ₃₀ H ₄₆ O ₄	470.33886	18.693	19747998.2703174	Triterpene saponin
Cryptotanshinone	96.8	C ₁₉ H ₂₀ O ₃	296.14049	18.947	181443226.025542	Diterpene
Daidzein	96.3	C ₁₅ H ₁₀ O ₄	254.05765	14.25	10265683.3609214	Isoflavones
Nicotinic acid	95.6	C ₆ H ₅ NO ₂	123.03215	2.293	47518158.8212902	Organic acid

RT, retention time.

acid (Table 3). Interestingly, the eight main compounds had antifibrotic roles. For example, ursolic acid from *Salvia miltiorrhiza* Bunge and *Glycyrrhiza uralensis* Fisch was reported to inhibit HSC activation, inflammasome pathways, and bacterial dysbiosis, which eventually reversed liver fibrosis progression (Yu et al., 2017; Nie et al., 2021). Formononetin from *Astragalus mongholicus* Bunge, *Glycyrrhiza uralensis* Fisch, and *Sparganium stolonierum* Buch was demonstrated to be an efficient component against liver fibrosis (Wang et al., 2021). Compound characteristics are presented in Table 3, mainly including mzCloud Best-Match score, formula, molecular weight, retention time, area, and classification. Overall, these identified compounds accounted for the potential antifibrotic effects of Qijia Rougan decoction.

Qijia Rougan Decoction Improves the Liver Index, Liver Function, and Serum Liver Fibrosis Index of CCl₄-Induced Rats

To identify the effects of Qijia Rougan decoction on liver index and serum biochemical indicators of fibrotic hepatic damage, we treated CCl₄-induced hepatic fibrosis rats with different Qijia Rougan decoction dosages (7.0 and 28 g/kg). The results showed that CCl₄ decreased the body weight and increased the liver weight of rats compared with that of controls (Figures 2A,B). Although Qijia Rougan decoction did not improve the body weight of rats induced by CCl₄, it decreased their liver weight (Figures 2A,B). Similarly, Qijia Rougan decoction improved the liver index of CCl₄-treated rats (Figure 2C).



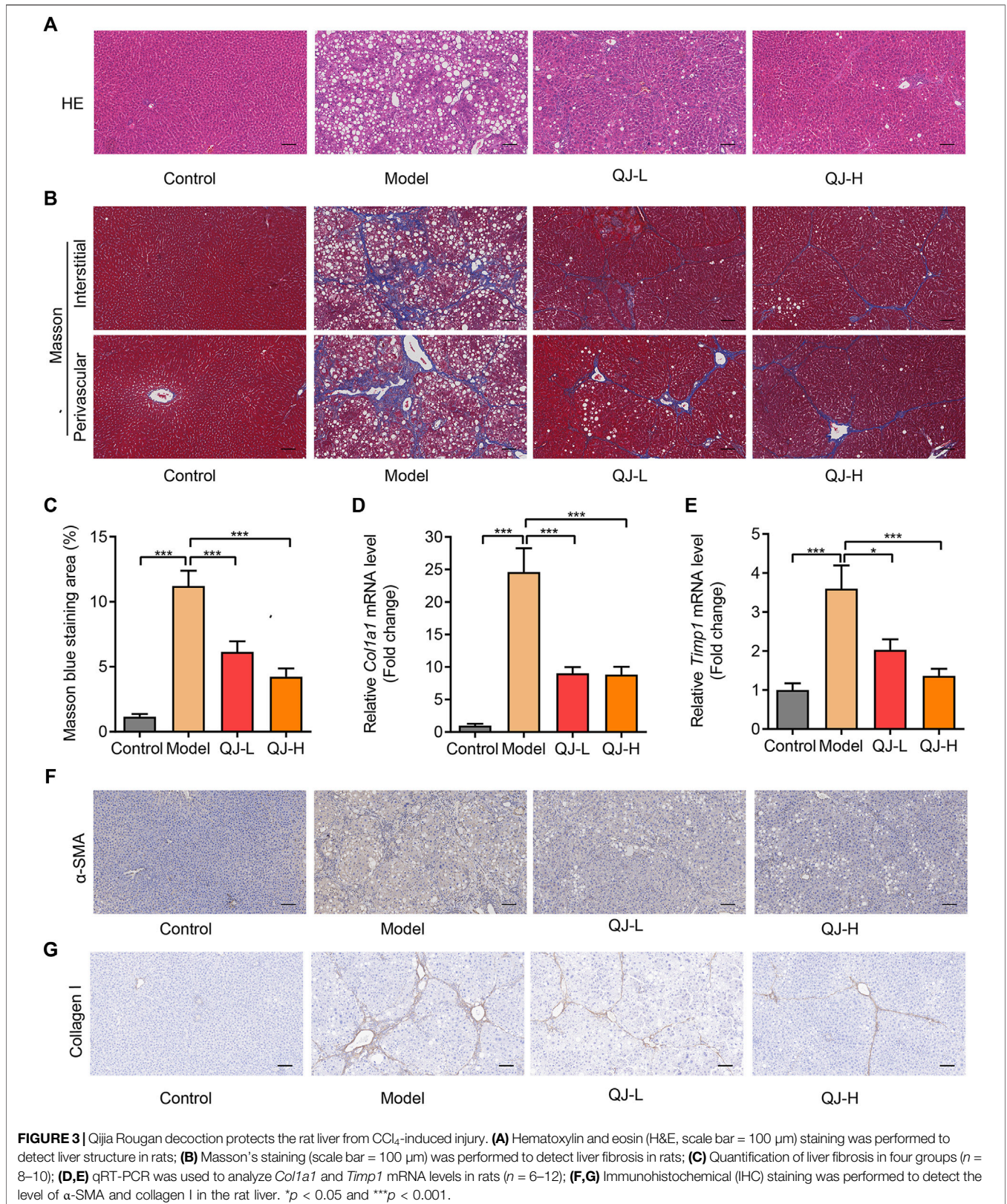
To validate the effect of Qijia Rougan decoction on CCl_4 -induced rat liver function, we detected the abundance of ALT, AST, and TBIL in the serum of rats. We observed a strong increase in ALT, AST, and TBIL levels in the blood of CCl_4 -induced rats, which was dramatically reduced by oral Qijia Rougan decoction treatment (Figures 2D–F). These findings indicated that Qijia Rougan decoction repressed the CCl_4 -induced increase of serum liver function indicators.

To further investigate the antifibrotic role of Qijia Rougan decoction, we detected HA, PC-III, and LN levels in the serum. Consistent with the serum liver function index, HA, PC-III, and LN serum levels were markedly increased in response to CCl_4 . However, these indexes were prominently reduced upon Qijia Rougan decoction treatment (Figures

2G–I). These results demonstrated that Qijia Rougan decoction alleviated the CCl_4 -induced increase in serum liver fibrosis indicators. Collectively, these findings indicated that Qijia Rougan decoction improved the CCl_4 -induced liver indexes and serum biochemical indicators.

Qijia Rougan Decoction Protects the Liver From Injury Induced by CCl_4 in Rats

To further evaluate the antifibrotic function of Qijia Rougan decoction, we measured the liver histopathological changes. Hematoxylin–eosin (H&E) staining was performed to detect the liver structure. Our results indicated significantly swollen and necrotic hepatocytes and inflammatory infiltration in



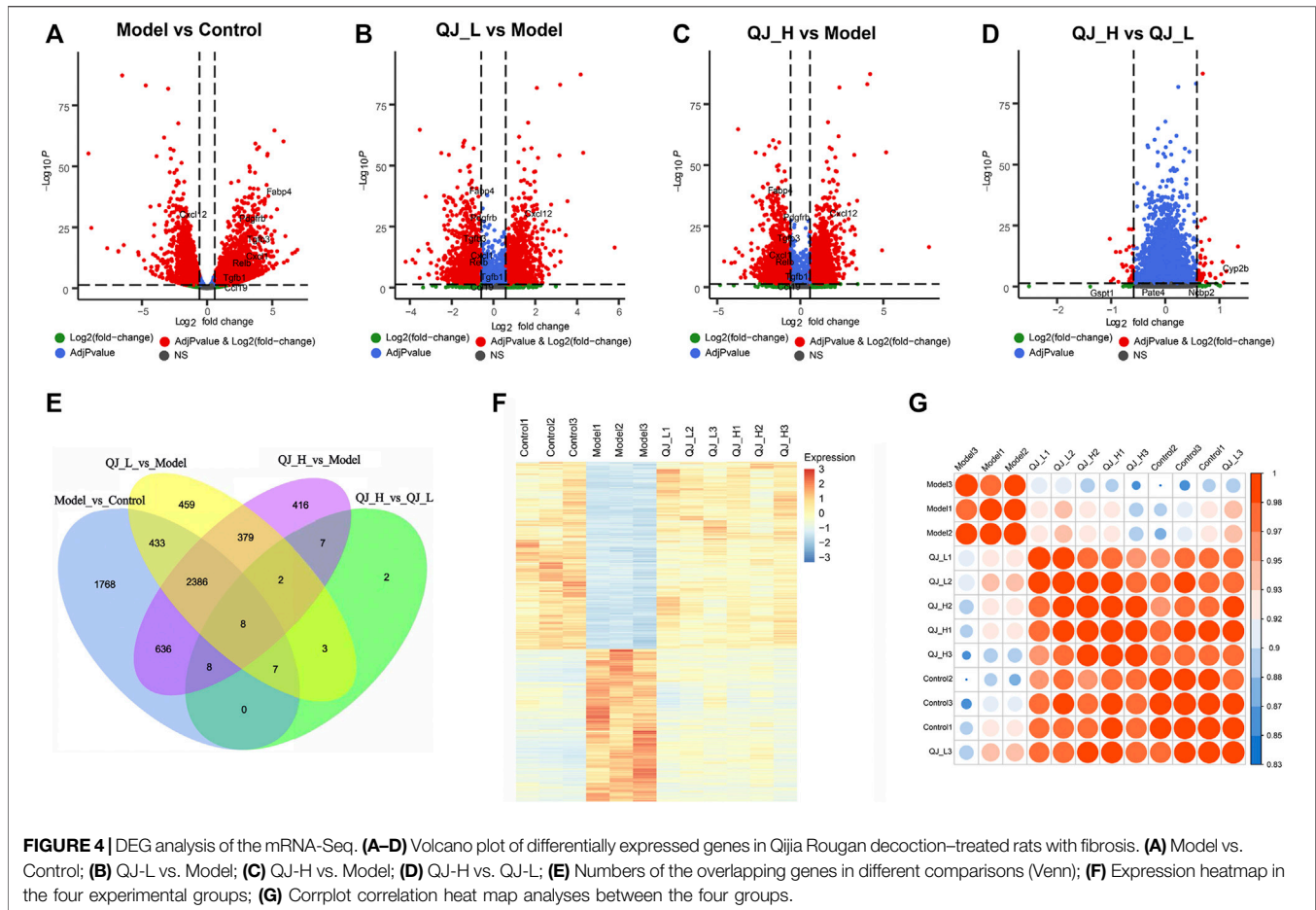


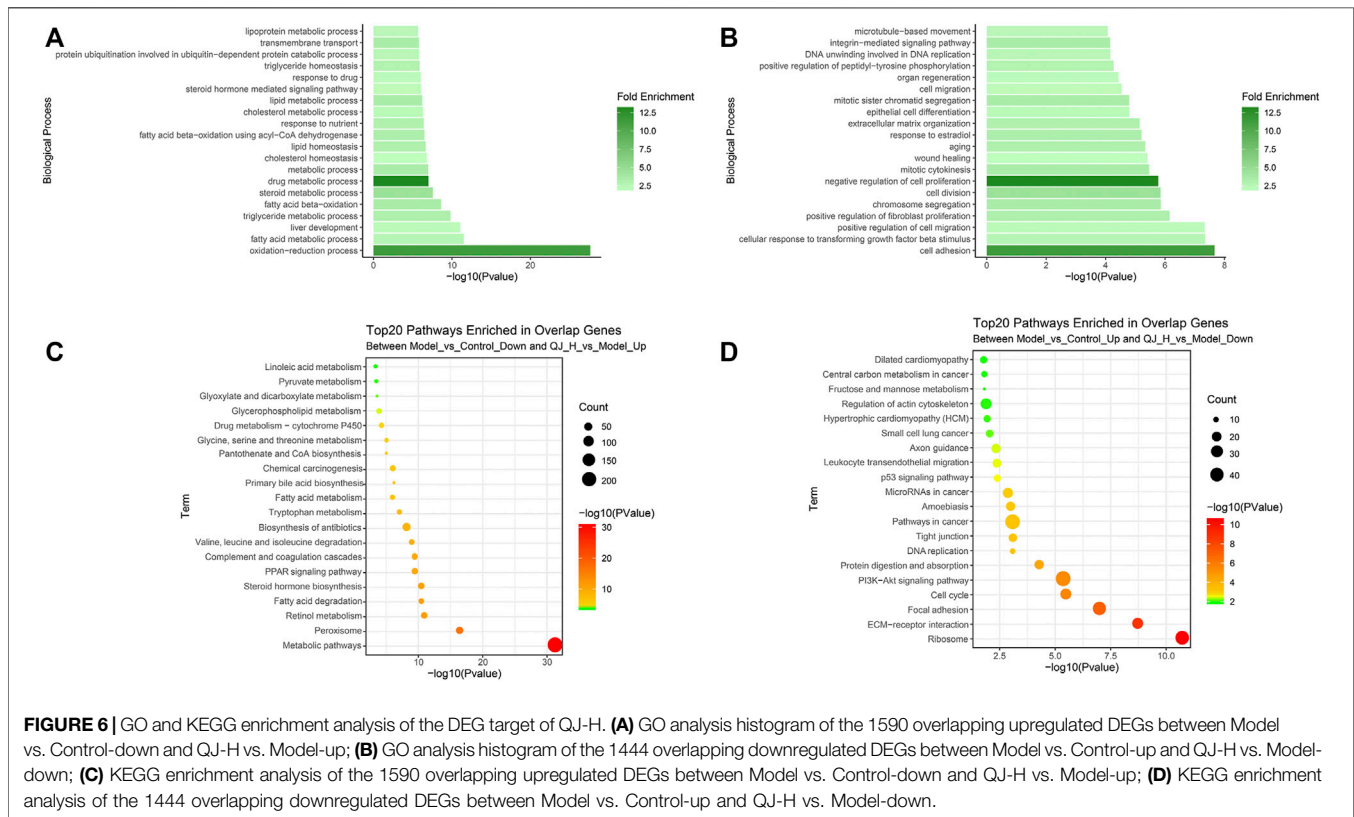
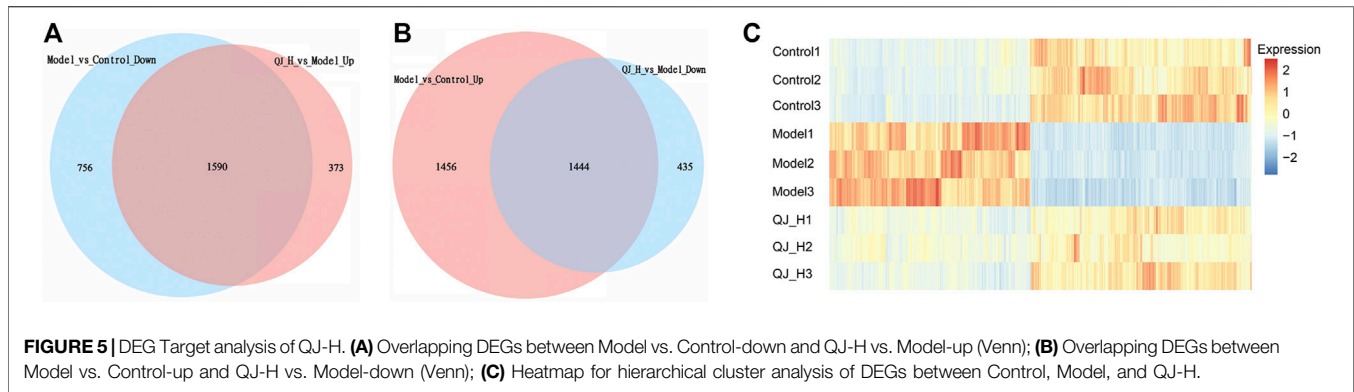
TABLE 4 | Differentially expressed genes in the different comparison groups.

Comparison group	Upregulated	Percentage (%)	Downregulated	Percentage (%)	Total DEGs
Model vs. control	2346	44.7	2900	55.3	5246
QJ-L vs. model	1969	53.5	1708	46.5	3677
QJ-H vs. model	1963	51.1	1879	48.9	3842
QJ-H vs. QJ-L	24	64.9	13	35.1	37

QJ-L, Qijia Rougan decoction low-dose group; QJ-H, Qijia Rougan decoction high-dose group; DEGs, differential expressed genes.

CCl_4 -induced rats when compared with controls. Conversely, these abnormalities were reversed in the liver of Qijia Rougan decoction–treated rats when compared with the models (**Figure 3A**). In addition, Masson’s staining showed that CCl_4 notably increased the formation of perivascular and interstitial fibrosis, while Qijia Rougan decoction alleviated these phenotypes (**Figures 3B,C**). Moreover, the mRNA expression of hepatic fibrosis markers, such as *Col1a1* and *Timp1*, was significantly increased in CCl_4 -induced rats and repressed by Qijia Rougan decoction treatment (**Figures 3D,E**). Furthermore, HSC activation is a hallmark of liver fibrosis, and α -SMA is a symbol of activated HSCs (Tsuchida and Friedman, 2017). Immunohistochemical (IHC) staining

demonstrated that α -SMA levels were markedly enhanced upon CCl_4 treatment compared to those in the control group, while Qijia Rougan decoction treatment significantly decreased them (**Figure 3F**), indicating that Qijia Rougan decoction can efficiently repress HSC activation. In addition, liver fibrosis is characterized by excessive deposition of extracellular matrix in the liver, and collagen I is the major extracellular matrix component. IHC staining results indicated that CCl_4 induction promoted the protein expression of collagen I, which was dramatically reduced by Qijia Rougan decoction treatment (**Figure 3G**), indicating that Qijia Rougan decoction significantly suppressed extracellular matrix formation. Collectively,



these findings suggested that Qijia Rougan decoction inhibited liver fibrosis progression.

Gene Expression Analysis by mRNA-Seq

To gain insight into liver transcriptional changes in response to Qijia Rougan decoction treatment, we performed mRNA-seq. We obtained 17294 genes, and differentially expressed genes (DEGs) were filtered based on p -value < 0.05 and absolute foldchange ≥ 1.5 . We detected 2,346 upregulated genes and 2,900 downregulated genes between the model and control groups, 1,969 upregulated genes and 1,708 downregulated genes in the comparison of QJ-L versus the model group, and 1,963 and 1,879

upregulated and downregulated genes, respectively, between QJ-H and the model group (Figures 4A–C; Table 4). Surprisingly, there were only 37 DEGs in comparison between the QJ-H and QJ-L groups, including 24 upregulated genes and 13 downregulated genes (Figure 4D; Table 4). The overlapping genes in the different groups are shown in Figure 4E. Interestingly, the expression tendencies of DEGs could be reversed by Qijia Rougan decoction treatment (Figure 4F). Notably, corplot correlation heat map analyses indicated that Qijia Rougan decoction treatment groups were closely correlated with the control group (Figure 4G). These data suggested the potential therapeutic benefits of Qijia Rougan decoction.

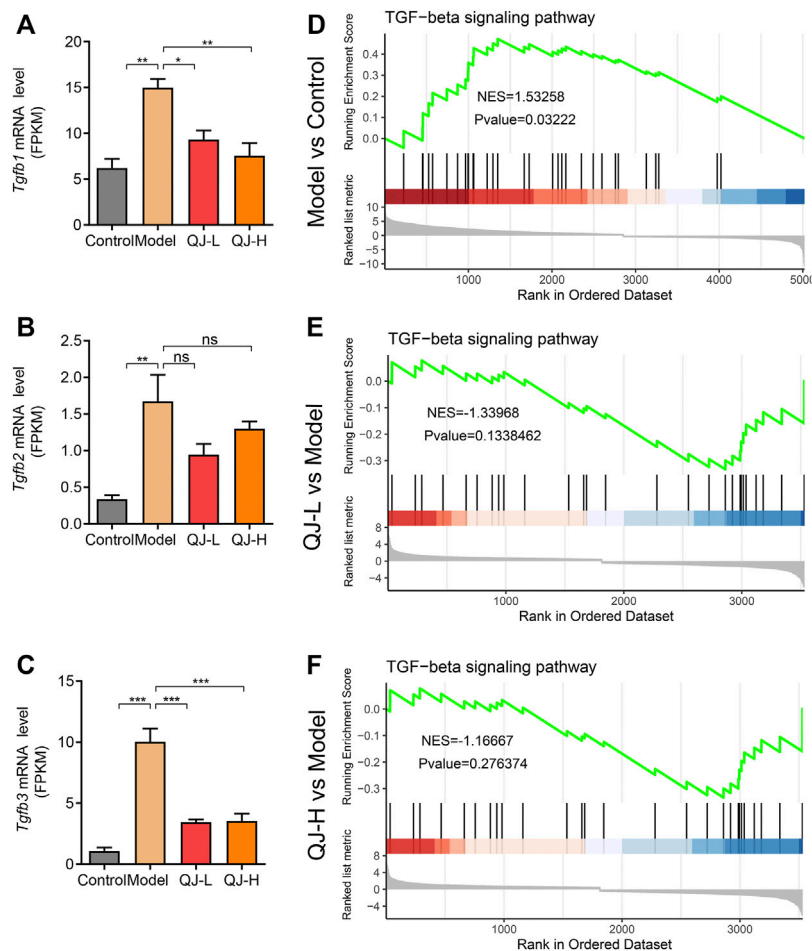


FIGURE 7 | Expression level and Gene Set Enrichment Analysis (GSEA) analysis of TGF-beta signaling. **(A–C)** Bulk RNA-seq analysis of the expression level of *Tgfb1*, *Tgfb2*, and *Tgfb3* ($n = 3$); **(D–F)** Gene Set Enrichment Analysis (GSEA) analysis of TGF-beta signaling. NES, normalized enrichment score; positive and negative NESs indicate higher and lower expression, respectively. * $p < 0.05$, ** $p < 0.01$, and *** $p < 0.001$. ns, not significant.

Target Gene Analysis of Qijia Rougan Decoction

To further elucidate the underlying action model of Qijia Rougan decoction (QJ) in liver fibrosis, we focused on the DEG target of QJ-H. Upregulated DEG target of QJ-H referred to the overlapping genes between Model-vs-Control-Down and QJ-H-vs-Model-Up, which were downregulated in the model group whereas upregulated in the QJ-H group, and the downregulated DEG target of QJ-H referred to the overlapping genes between Model-vs-Control-Up and QJ-H-vs-Model-Down, which were highly expressed in the model group whereas lowly expressed in the QJ-H group. We identified 1,590 upregulated and 1,444 downregulated DEG targets in QJ-H (Figures 5A,B). Surprisingly, the abovementioned DEG target showed remarkable differences between groups, and the disturbance induced by CCl_4 in the model group could be rebalanced by Qijia Rougan decoction in the QJ-H group (Figure 5C). Similarly, 1,482 upregulated and 1,341 downregulated DEG targets in QJ-L were identified

(Supplementary Figures S1A,B), and the expression tendencies of DEG targets in QJ-L were consistent with those in QJ-H (Supplementary Figure S1C).

Gene Ontology and Kyoto Encyclopedia of Genes and Genomes Enrichment Analysis on Differentially Expressed Gene Target of Qijia Rougan Decoction

To clarify the functions and signaling cascades enriched upon Qijia Rougan decoction treatment in CCl_4 -induced liver fibrosis, 1,590 upregulated and 1,444 downregulated DEG targets of QJ-H were used for Gene Ontology (GO) and Kyoto Encyclopedia of Genes and Genomes (KEGG) enrichment analysis. GO analysis indicated that upregulated DEG targets of QJ-H were involved in the oxidation–reduction process, fatty acid metabolism, liver development, and triglyceride metabolism (Figure 6A). Downregulated DEG targets of QJ-H primarily participated in biological processes including cell adhesion, TGF β signaling, positive regulation of cell migration, and positive regulation of

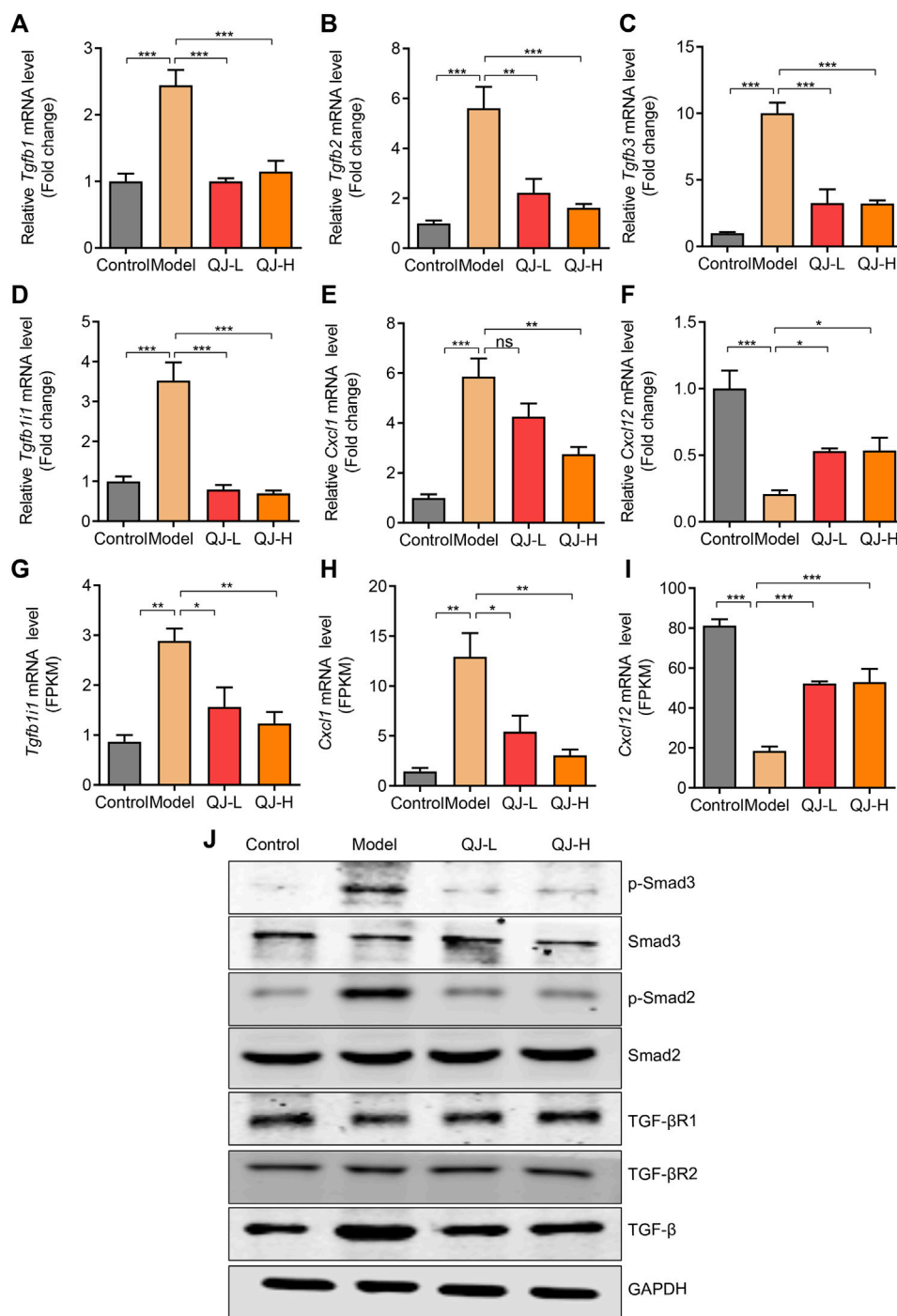


FIGURE 8 | Validation of the expression of mRNA and proteins. **(A–F)** qRT-PCR validations of related genes ($n = 4$): **(A)** *Tgfb1*: transforming growth factor beta 1; **(B)** *Tgfb2*: transforming growth factor, beta 2; **(C)** *Tgfb3*: transforming growth factor beta 3; **(D)** *Tgfb1i1*: transforming growth factor beta 1-induced transcript 1; **(E)** *Cxcl1*: C-X-C motif chemokine ligand 1; **(F)** *Cxcl12*: C-X-C motif chemokine ligand 12; **(G–I)** Bulk RNA-seq analysis of the expression level of *Tgfb1i1*, *Cxcl1*, and *Cxcl12* ($n = 3$); **(J)** Representative Western blotting was performed to detect the levels of p-Smad3, Smad3, p-Smad2, Smad2, TGF- β 1, TGF- β 2, and TGF- β .

fibroblast proliferation (**Figure 6B**). KEGG analysis suggested that upregulated DEG targets of QJ-H were closely related to metabolism pathways including peroxisome, retinol metabolism,

fatty acid degradation, and steroid hormone biosynthesis (**Figure 6C**). Conversely, downregulated DEG targets of QJ-H were mainly associated with ribosome, ECM-receptor

interactions, focal adhesions, and the cell cycle (Figure 6D). GO and KEGG enrichment analysis results of DEG target in QJ-L were similar to those in QJ-H (Supplementary Figures S2A–D).

Qijia Rougan Decoction Molecular Mechanism Analysis

Accumulating evidence has demonstrated the profibrogenic effect of TGF β signaling (Fabregat et al., 2016; Sun et al., 2021). In GO enrichment analyses, we observed the significant enrichment of TGF β in the downregulated DEG target of QJ (Figure 6B; Supplementary Figure S2B). Bulk RNA-seq analyses also showed the increased expression of three TGF β isoforms (*Tgfb1*, *Tgfb2*, and *Tgfb3*), especially the *Tgfb1* and *Tgfb3*, after CCl₄ injection, along with its decrease upon Qijia Rougan decoction treatment (Figures 7A–C). To further explore the role of TGF β signaling, we also analyzed the differential expression of TGF β signaling pathway components between CCl₄ and Qijia Rougan decoction treatment using Gene Set Enrichment Analysis (GSEA) based on the abovementioned data. Notably, we found that TGF β signaling was remarkably activated in response to CCl₄ (Figure 7D), whereas low- or high-dose Qijia Rougan decoction inhibited it (Figures 7E,F). These data indicated that Qijia Rougan decoction exerted a protective role in liver fibrosis, at least in part, through TGF β signaling.

To validate our results, we detected the expression of several genes associated with the TGF β signaling pathway using qRT-PCR. Consistent with mRNA-seq results, three TGF β isoforms (*Tgfb1*, *Tgfb2*, and *Tgfb3*) showed increased expression in the model group, and Qijia Rougan decoction could decrease their levels (Figures 8A–C). The expression pattern of *Tgfb1i1*, a gene induced by TGF β , was similar to that of TGF β isoforms (Figures 8D,G). Furthermore, Western blotting results showed Qijia Rougan decoction did not influence the expression of TGF- β receptors I and II. But CCl₄ injection induced the activation of the TGF- β and its classical downstream Smad2 and Smad3 proteins, while Qijia Rougan decoction could inhibit the activation of the TGF β signaling pathway (Figure 8J). In addition, the inflammatory response is an important contributor to liver fibrosis. Therefore, we also detected inflammatory factor expression and found that Qijia Rougan decoction could also modulate inflammatory responses, supported by increased inflammatory *Cxcl1* cytokine levels and decreased inflammatory *Cxcl12* chemokine levels in CCl₄-induced rats, which were reversed by Qijia Rougan decoction (Figures 8E,F,H,I). Collectively, these findings indicated that Qijia Rougan decoction protected the fibrotic liver by inhibiting TGF β signaling and modulating inflammation responses.

DISCUSSION

Owing to a lack of effective drugs to treat liver fibrosis, diseases associated with liver fibrosis have become a serious health threat worldwide. TCM holds great potential to tackle this health burden. In the present study, we found that Qijia Rougan decoction exerted a hepatoprotective role in liver fibrosis. We

found that CCl₄ significantly enhanced the formation of liver fibrosis, manifesting as large numbers of apoptotic hepatocytes, collagen accumulation, severe inflammatory infiltration, and the activation of inflammatory factors and inflammatory signaling pathways. Oral Qijia Rougan decoction attenuated these phenotypes by inhibiting TGF β signaling and inflammatory responses. These data suggest the therapeutic effect of Qijia Rougan decoction on liver fibrosis.

Patients subjected to early liver fibrosis generally have no symptoms, while its early detection and treatment could strongly prevent its deterioration to cirrhosis and hepatic carcinoma, improving the survival and quality of life of patients (Zhang and Friedman, 2012). Clinicians could diagnose a patient with liver fibrosis based on liver biopsy in the preceding decades (Liu et al., 2019). Due to its invasiveness and sample error, the non-invasive detection of hepatic fibrosis is more practical (Wong, 2018; Liu et al., 2019). ALT, AST, and TBIL are important indicators for assessing liver function (Qiao and Zhao, 2021). Qijia Rougan decoction was shown to inhibit the increased levels of serum ALT, AST, and TBIL induced by CCl₄, indicating that it significantly protected liver integrity. In addition, the degree of liver fibrosis is also classified by the abundance of serum liver fibrosis indicators, including HA, LN, PCIII, and IV-C (Ma et al., 2021; Qiao and Zhao, 2021). Qijia Rougan decoction was demonstrated to reverse the enhanced HA, LN, and PCIII levels, suggesting its antifibrotic effects. We conclude that Qijia Rougan decoction is a hepatoprotective TCM formula.

TCM preparations often show multiple components and multiple targets (Wu et al., 2021; Xue et al., 2021). Over 1,000 ingredients were identified in the Qijia Rougan decoction via HPLC-MS/MS analysis. Many ingredients derived from raw herbs and animal drugs in the Qijia Rougan decoction were reported to possess antifibrotic effects. For example, formononetin, a common component of *Astragalus mongholicus* Bunge, *Glycyrrhiza uralensis* Fisch., and *Sparganium stolonierum*, Buch., was proven to be efficient against liver fibrosis (Wang et al., 2021). It also inhibited cholestasis, a precursor of liver fibrosis, partly by increasing the expression of SIRT1 to activate the PPAR α , which eventually maintained bile acid metabolism and reduced inflammatory reactions (Yang et al., 2019). These data support the antifibrotic effect of Qijia Rougan decoction. Furthermore, ursolic acid, a pentacyclic triterpenoid, rich in *Salvia miltiorrhiza* Bunge and *Glycyrrhiza uralensis* Fisch., found in the Qijia Rougan decoction, reportedly possessed excellent antioxidative, anti-inflammatory, and antifibrotic effects (Wan et al., 2019; Nie et al., 2021). A series of published studies have demonstrated the significant protective role of ursolic acid against liver fibrosis and mechanical insights ranging from the inhibition of hepatic stellate cell (HSC) activation (Wang et al., 2011; Yu et al., 2017), hepatic circadian rhythm regulation (Kwon et al., 2018), and gut dysbiosis improvement (Wan et al., 2019; Wan et al., 2020) to NADPH oxidase 4 (NOX4)/NOD-like receptor protein 3 (NLRP3) inflammasome pathway suppression (Nie et al., 2021) and oxidative stress repression through LKB1-AMPK signaling activation (Yang et al., 2015). Another main component derived from *Salvia miltiorrhiza* Bunge, called

Tanshinone IIA, was also reported to have therapeutic potential for treating liver fibrosis (Ying et al., 2019), as it might inhibit HSC proliferation and extracellular matrix deposition (Shi et al., 2020). More interestingly, other main components identified in Qijia Rougan decoction, such as isoliquiritigenin, glycyrrhetic acid, and daidzein, were demonstrated to have excellent antifibrotic activity (Chen et al., 2013; Soumyakrishnan et al., 2014; Wang et al., 2021). Therefore, the components present in Qijia Rougan decoction may synergistically mediate its hepatoprotective functions.

TGF β , a central contributor of fibrogenesis, has been widely studied in liver fibrosis (Fabregat et al., 2016; Sun et al., 2021). TGF- β 1, TGF- β 2, and TGF- β 3 belong to the TGF β superfamily, and all play essential roles in fibrotic disease pathogenesis (Sun et al., 2021). In general, TGF- β 1 is the most widely and deeply studied subtype in the formation of liver fibrosis (Fan et al., 2019; Xu et al., 2020). It is considered that activation of TGF- β 1 could accelerate the progression of liver fibrosis by activating hepatic stellate cells (HSCs) (Li Y. et al., 2022). Activated HSCs are characterized by increased α -SMA expression. Mechanistically, TGF β activates HSCs and increases extracellular matrix (ECM) deposition, which promotes liver fibrosis (Dewidar et al., 2019). In our study, we observed increased levels of α -SMA induced by CCl₄ which decreased upon Qijia Rougan decoction treatment. Meanwhile, collagen I, the dominating component of the extracellular matrix, was prominently improved by Qijia Rougan decoction. The canonical TGF β signaling pathway is dependent on the downstream of Smad proteins, including Smad2 and Smad3 (Dewidar et al., 2019; Chen et al., 2021). Surprisingly, in this study, the canonical TGF β signaling pathway was activated along with an enhancement of three TGF β isoforms (*Tgfb1*, *Tgfb2*, and *Tgfb3*) in the fibrotic liver. Upon Qijia Rougan decoction treatment, TGF β signaling was repressed and the expression of *Tgfb1*, *Tgfb2*, and *Tgfb3* decreased. Collectively, TGF β signaling inhibition may be a core mechanism underlying the Qijia Rougan decoction-mediated hepatoprotective functions.

In conclusion, we demonstrated the value of Qijia Rougan decoction as a hepatoprotective TCM. Qijia Rougan decoction prevented CCl₄-induced hepatocyte damage and fibrotic liver injury by modulating inflammatory responses and TGF β signaling. These results indicate that Qijia Rougan

decoction and its bioactive components are potential therapeutic options for treating liver fibrosis in clinical practice.

DATA AVAILABILITY STATEMENT

The datasets presented in this study can be found in online repositories. The names of the repository/repositories and accession number(s) can be found below: <https://www.ncbi.nlm.nih.gov/PRJNA826993>.

ETHICS STATEMENT

The animal study was reviewed and approved by Ethics Committee of Chengdu University of Traditional Chinese Medicine.

AUTHOR CONTRIBUTIONS

CL and HY conceived and supervised the study. X-FC, YW, SJ, XS, and QF performed the experiments and informatic analysis. X-FC, CL, and HY drafted and revised the manuscript. All authors have read and approved the final manuscript.

FUNDING

This work was supported by grants from the National Natural Science Foundation of China (No. 82004097), the China Postdoctoral Science Foundation (No. 2020M673163), and the Potential Postdoctoral Program of Chengdu University of Traditional Chinese Medicine (No. BSH2019015).

SUPPLEMENTARY MATERIAL

The Supplementary Material for this article can be found online at: <https://www.frontiersin.org/articles/10.3389/fphar.2022.911250/full#supplementary-material>

REFERENCES

- Ali, M., Khan, T., Fatima, K., Ali, Q. U. A., Ovais, M., Khalil, A. T., et al. (2018). Selected Hepatoprotective Herbal Medicines: Evidence from Ethnomedicinal Applications, Animal Models, and Possible Mechanism of Actions. *Phytother. Res.* 32 (2), 199–215. doi:10.1002/ptr.5957
- Chen, S., Zou, L., Li, L., and Wu, T. (2013). The Protective Effect of Glycyrrhetic Acid on Carbon Tetrachloride-Induced Chronic Liver Fibrosis in Mice via Upregulation of Nrf2. *PLoS One* 8 (1), e53662. doi:10.1371/journal.pone.0053662
- Chen, H., Cai, J., Wang, J., Qiu, Y., Jiang, C., Wang, Y., et al. (2021). Targeting Nestin⁺ Hepatic Stellate Cells Ameliorates Liver Fibrosis by Facilitating T β RI Degradation. *J. Hepatol.* 74 (5), 1176–1187. doi:10.1016/j.jhep.2020.11.016
- Dewidar, B., Meyer, C., Dooley, S., and Meindl-Beinker, A. N. (2019). TGF- β in Hepatic Stellate Cell Activation and Liver Fibrogenesis-Updated 2019. *Cells* 8 (11), 1419. doi:10.3390/cells8111419
- Fabregat, I., Moreno-Càceres, J., Sánchez, A., Dooley, S., Dewidar, B., Giannelli, G., et al. (2016). TGF- β Signalling and Liver Disease. *FEBS J.* 283 (12), 2219–2232. doi:10.1111/febs.13665
- Fan, W., Liu, T., Chen, W., Hammad, S., Longerich, T., Hausser, I., et al. (2019). ECM1 Prevents Activation of Transforming Growth Factor β , Hepatic Stellate Cells, and Fibrogenesis in Mice. *Gastroenterology* 157 (5), 1352. doi:10.1053/j.gastro.2019.07.036
- Feng, Y., Cheung, K. F., Wang, N., Liu, P., Nagamatsu, T., and Tong, Y. (2009). Chinese Medicines as a Resource for Liver Fibrosis Treatment. *Chin. Med.* 4, 16. doi:10.1186/1749-8546-4-16
- Friedman, S. L., and Pinzani, M. (2022). Hepatic Fibrosis 2022: Unmet Needs and a Blueprint for the Future. *Hepatology* 75 (2), 473–488. doi:10.1002/hep.32285

- Gao, J., Wei, B., de Assuncao, T. M., Liu, Z., Hu, X., Ibrahim, S., et al. (2020). Hepatic Stellate Cell Autophagy Inhibits Extracellular Vesicle Release to Attenuate Liver Fibrosis. *J. Hepatol.* 73 (5), 1144–1154. doi:10.1016/j.jhep.2020.04.044
- Hu, Z., You, P., Xiong, S., Gao, J., Tang, Y., Ye, X., et al. (2017). Carapax Trionycis Extracts Inhibit Fibrogenesis of Activated Hepatic Stellate Cells via TGF- β 1/Smad and NF κ B Signaling. *Biomed. Pharmacother.* 95, 11–17. doi:10.1016/j.biopha.2017.08.011
- Kisseleva, T., and Brenner, D. (2021). Molecular and Cellular Mechanisms of Liver Fibrosis and its Regression. *Nat. Rev. Gastroenterol. Hepatol.* 18 (3), 151–166. doi:10.1038/s41575-020-00372-7
- Kwon, E. Y., Shin, S. K., and Choi, M. S. (2018). Ursolic Acid Attenuates Hepatic Steatosis, Fibrosis, and Insulin Resistance by Modulating the Circadian Rhythm Pathway in Diet-Induced Obese Mice. *Nutrients* 10 (11), 1719. doi:10.3390/nu10111719
- Li, G., Zhou, Y., Sze, D. M., Liu, C., Zhang, Q., Wang, Z., et al. (2019). Active Ingredients and Action Mechanisms of Yi Guan Jian Decoction in Chronic Hepatitis B Patients with Liver Fibrosis. *Evid. Based Complement. Altern. Med.* 2019, 2408126. doi:10.1155/2019/2408126
- Li, X., Yu, H., Gong, Y., Wu, P., Feng, Q., and Liu, C. (2022a). Fuzheng Xiaozheng Prescription Relieves Rat Hepatocellular Carcinoma through Improving Anti-inflammation Capacity and Regulating Lipid Related Metabolisms. *J. Ethnopharmacol.* 284, 114801. doi:10.1016/j.jep.2021.114801
- Li, Y., Fan, W., Link, F., Wang, S., and Dooley, S. (2022b). Transforming Growth Factor β Latency: A Mechanism of Cytokine Storage and Signalling Regulation in Liver Homeostasis and Disease. *JHEP Rep.* 4 (2), 100397. doi:10.1016/j.jhep.2021.100397
- Li, H. (2020). Advances in Anti Hepatic Fibrotic Therapy with Traditional Chinese Medicine Herbal Formula. *J. Ethnopharmacol.* 251, 112442. doi:10.1016/j.jep.2019.112442
- Liu, Y. T., and Lv, W. L. (2020). Research Progress in Astragalus Membranaceus and its Active Components on Immune Responses in Liver Fibrosis. *Chin. J. Integr. Med.* 26 (10), 794–800. doi:10.1007/s11655-019-3039-1
- Liu, L., Cao, J., Zhong, Z., Guo, Z., Jiang, Y., Bai, Y., et al. (2019). Noninvasive Indicators Predict Advanced Liver Fibrosis in Autoimmune Hepatitis Patients. *J. Clin. Lab. Anal.* 33 (7), e22922. doi:10.1002/jcla.22922
- Ma, H. Y., Dong, L., Quan, S. Z., Li, R. Y., and Wang, X. R. (2021). Comparison of Four Markers of Hepatic Fibrosis and Hepatic Function Indices in Patients with Liver Cirrhosis and Hepatoma. *Ann. Palliat. Med.* 10 (4), 4108–4121. doi:10.21037/apm-20-1623
- Mu, M., Zuo, S., Wu, R. M., Deng, K. S., Lu, S., Zhu, J. J., et al. (2018). Ferulic Acid Attenuates Liver Fibrosis and Hepatic Stellate Cell Activation via Inhibition of TGF- β /Smad Signaling Pathway. *Drug Des. Devel Ther.* 12, 4107–4115. doi:10.2147/ddt.S186726
- Nie, Y., Liu, Q., Zhang, W., Wan, Y., Huang, C., and Zhu, X. (2021). Ursolic Acid Reverses Liver Fibrosis by Inhibiting NOX4/NLRP3 Inflammasome Pathways and Bacterial Dysbiosis. *Gut Microbes* 13 (1), 1972746. doi:10.1080/19490976.2021.1972746
- Parola, M., and Pinzani, M. (2019). Liver Fibrosis: Pathophysiology, Pathogenetic Targets and Clinical Issues. *Mol. Asp. Med.* 65, 37–55. doi:10.1016/j.mam.2018.09.002
- Pellicoro, A., Ramachandran, P., Iredale, J. P., and Fallowfield, J. A. (2014). Liver Fibrosis and Repair: Immune Regulation of Wound Healing in a Solid Organ. *Nat. Rev. Immunol.* 14 (3), 181–194. doi:10.1038/nri3623
- Qiao, J., and Zhao, C. (2021). Therapeutic Effect of Adenosylmethionine on Viral Hepatitis and Related Factors Inducing Diseases. *Am. J. Transl. Res.* 13 (8), 9485–9494.
- Schuppan, D., Ashfaq-Khan, M., Yang, A. T., and Kim, Y. O. (2018). Liver Fibrosis: Direct Antifibrotic Agents and Targeted Therapies. *Matrix Biol.* 68–69, 435–451. doi:10.1016/j.matbio.2018.04.006
- Schwabe, R. F., Tabas, I., and Pajvani, U. B. (2020). Mechanisms of Fibrosis Development in Nonalcoholic Steatohepatitis. *Gastroenterology* 158 (7), 1913–1928. doi:10.1053/j.gastro.2019.11.311
- Shi, M. J., Yan, X. L., Dong, B. S., Yang, W. N., Su, S. B., and Zhang, H. (2020). A Network Pharmacology Approach to Investigating the Mechanism of Tanshinone IIA for the Treatment of Liver Fibrosis. *J. Ethnopharmacol.* 253, 112689. doi:10.1016/j.jep.2020.112689
- Soumyakrishnan, S., Divya, T., Kalayarasan, S., Sriram, N., and Sudhandiran, G. (2014). Daidzein Exhibits Anti-fibrotic Effect by Reducing the Expressions of Proteinase Activated Receptor 2 and TGF β 1/smcd Mediated Inflammation and Apoptosis in Bleomycin-Induced Experimental Pulmonary Fibrosis. *Biochimie* 103, 23–36. doi:10.1016/j.biochi.2014.04.005
- Sun, T., Huang, Z., Liang, W. C., Yin, J., Lin, W. Y., Wu, J., et al. (2021). TGF β 2 and TGF β 3 Isoforms Drive Fibrotic Disease Pathogenesis. *Sci. Transl. Med.* 13 (605), eabe0407. doi:10.1126/scitranslmed.abe0407
- Tan, Y., Lv, Z. P., Bai, X. C., Liu, X. Y., and Zhang, X. F. (2006). Traditional Chinese Medicine Bao Gan Ning Increase Phosphorylation of CREB in Liver Fibrosis *In Vivo* and *In Vitro*. *J. Ethnopharmacol.* 105 (1–2), 69–75. doi:10.1016/j.jep.2005.09.040
- Tang, X., Chen, X. F., Wang, N. Y., Wang, X. M., Liang, S. T., Zheng, W., et al. (2017). SIRT2 Acts as a Cardioprotective Deacetylase in Pathological Cardiac Hypertrophy. *Circulation* 136 (21), 2051–2067. doi:10.1161/circulationaha.117.028728
- Tsuchida, T., and Friedman, S. L. (2017). Mechanisms of Hepatic Stellate Cell Activation. *Nat. Rev. Gastroenterol. Hepatol.* 14 (7), 397–411. doi:10.1038/nrgastro.2017.38
- Wan, S. Z., Liu, C., Huang, C. K., Luo, F. Y., and Zhu, X. (2019). Ursolic Acid Improves Intestinal Damage and Bacterial Dysbiosis in Liver Fibrosis Mice. *Front. Pharmacol.* 10, 1321. doi:10.3389/fphar.2019.01321
- Wan, S., Huang, C., Wang, A., and Zhu, X. (2020). Ursolic Acid Improves the Bacterial Community Mapping of the Intestinal Tract in Liver Fibrosis Mice. *PeerJ* 8, e9050. doi:10.7717/peerj.9050
- Wang, X., Ikejima, K., Kon, K., Arai, K., Aoyama, T., Okumura, K., et al. (2011). Ursolic Acid Ameliorates Hepatic Fibrosis in the Rat by Specific Induction of Apoptosis in Hepatic Stellate Cells. *J. Hepatol.* 55 (2), 379–387. doi:10.1016/j.jhep.2010.10.040
- Wang, Y., Li, Y., Zhang, H., Zhu, L., Zhong, J., Zeng, J., et al. (2021). Pharmacokinetics-based Comprehensive Strategy to Identify Multiple Effective Components in Huangqi Decoction against Liver Fibrosis. *Phytomedicine* 84, 153513. doi:10.1016/j.phymed.2021.153513
- Wong, G. L. (2018). Non-invasive Assessments for Liver Fibrosis: The Crystal Ball We Long for. *J. Gastroenterol. Hepatol.* 33 (5), 1009–1015. doi:10.1111/jgh.14103
- Wu, W., Li, L., Yang, J., Li, P., Hu, Y., Zhang, G., et al. (2021). Therapeutic Effect of Biejiaxiaozheng Pills on Carbon Tetrachloride-Induced Hepatic Fibrosis in Rats through the NF- κ B/Nrf2 Pathway. *Gastroenterol. Res. Pract.* 2021, 3954244. doi:10.1155/2021/3954244
- Xu, M., Xu, H. H., Lin, Y., Sun, X., Wang, L. J., Fang, Z. P., et al. (2019). LECT2, a Ligand for Tie1, Plays a Crucial Role in Liver Fibrogenesis. *Cell* 178 (6), 1478. doi:10.1016/j.cell.2019.07.021
- Xu, Y., Sun, X., Zhang, R., Cao, T., Cai, S. Y., Boyer, J. L., et al. (2020). A Positive Feedback Loop of TET3 and TGF- β 1 Promotes Liver Fibrosis. *Cell Rep.* 30 (5), 1310. doi:10.1016/j.celrep.2019.12.092
- Xu, Y., Xu, W., Liu, W., Chen, G., Jiang, S., Chen, J., et al. (2021). Yiguanjian Decoction Inhibits Macrophage M1 Polarization and Attenuates Hepatic Fibrosis Induced by CCl4/2-AAF. *Pharm. Biol.* 59 (1), 1150–1160. doi:10.1080/13880209.2021.1961820
- Xue, X., Wu, J., Ding, M., Gao, F., Zhou, F., Xu, B., et al. (2021). Si-Wu-Tang Ameliorates Fibrotic Liver Injury via Modulating Intestinal Microbiota and Bile Acid Homeostasis. *Chin. Med.* 16 (1), 112. doi:10.1186/s13020-021-00524-0
- Yang, Y., Yang, S., Chen, M., Zhang, X., Zou, Y., and Zhang, X. (2008). Compound Astragalus and Salvia Miltiorrhiza Extract Exerts Anti-fibrosis by Mediating TGF- β /Smad Signaling in Myofibroblasts. *J. Ethnopharmacol.* 118 (2), 264–270. doi:10.1016/j.jep.2008.04.012
- Yang, Y., Zhao, Z., Liu, Y., Kang, X., Zhang, H., and Meng, M. (2015). Suppression of Oxidative Stress and Improvement of Liver Functions in Mice by Ursolic Acid via LKB1-AMP-Activated Protein Kinase Signaling. *J. Gastroenterol. Hepatol.* 30 (3), 609–618. doi:10.1111/jgh.12723
- Yang, S., Wei, L., Xia, R., Liu, L., Chen, Y., Zhang, W., et al. (2019). Formononetin Ameliorates Cholestasis by Regulating Hepatic SIRT1 and PPAR α . *Biochem. Biophys. Res. Commun.* 512 (4), 770–778. doi:10.1016/j.bbrc.2019.03.131
- Ying, Q., Teng, Y., Zhang, J., Cai, Z., and Xue, Z. (2019). Therapeutic Effect of Tanshinone IIA on Liver Fibrosis and the Possible Mechanism: A Preclinical Meta-Analysis. *Evid. Based Complement. Altern. Med.* 2019, 7514046. doi:10.1155/2019/7514046
- Yu, S. S., Chen, B., Huang, C. K., Zhou, J. J., Huang, X., Wang, A. J., et al. (2017). Ursolic Acid Suppresses TGF- β 1-Induced Quiescent HSC Activation and

- Transformation by Inhibiting NADPH Oxidase Expression and Hedgehog Signaling. *Exp. Ther. Med.* 14 (4), 3577–3582. doi:10.3892/etm.2017.5001
- Zhang, D. Y., and Friedman, S. L. (2012). Fibrosis-dependent Mechanisms of Hepatocarcinogenesis. *Hepatology* 56 (2), 769–775. doi:10.1002/hep.25670
- Zhao, J., Miao, J., Wei, X., Guo, L., Li, P., Lei, J., et al. (2021). Traditional Chinese Medicine Ganshuang Granules Attenuate CCl₄-Induced Hepatic Fibrosis by Modulating Gut Microbiota. *Chem. Biodivers.* 18 (11), e2100520. doi:10.1002/cbdv.202100520
- Zhou, Y. N., Mu, Y. P., Fu, W. W., Ning, B. B., Du, G. L., Chen, J. M., et al. (2015). Yiguanjian Decoction and its Ingredients Inhibit Angiogenesis in Carbon Tetrachloride-Induced Cirrhosis Mice. *BMC Complement. Altern. Med.* 15, 342. doi:10.1186/s12906-015-0862-6
- Zhou, Y., Wu, R., Cai, F. F., Zhou, W. J., Lu, Y. Y., Zhang, H., et al. (2021). Xiaoyaosan Decoction Alleviated Rat Liver Fibrosis via the TGF β /Smad and Akt/FoxO3 Signaling Pathways Based on Network Pharmacology Analysis. *J. Ethnopharmacol.* 264, 113021. doi:10.1016/j.jep.2020.113021

Conflict of Interest: The authors declare that the research was conducted in the absence of any commercial or financial relationships that could be construed as a potential conflict of interest.

Publisher's Note: All claims expressed in this article are solely those of the authors and do not necessarily represent those of their affiliated organizations, or those of the publisher, the editors, and the reviewers. Any product that may be evaluated in this article, or claim that may be made by its manufacturer, is not guaranteed or endorsed by the publisher.

Copyright © 2022 Chen, Wang, Ji, Sun, Feng, Yu and Liu. This is an open-access article distributed under the terms of the Creative Commons Attribution License (CC BY). The use, distribution or reproduction in other forums is permitted, provided the original author(s) and the copyright owner(s) are credited and that the original publication in this journal is cited, in accordance with accepted academic practice. No use, distribution or reproduction is permitted which does not comply with these terms.